

# PID CONTROLLER TUNED BY METAHEURISTIC ALGORITHM USING ANT LION OPTIMIZER FOR VIBRATION CONTROL OF HORIZONTAL FLEXIBLE STRUCTURE

Muhamad Sukri Hadi<sup>a\*</sup>, Aida Nur Syafiqah Shaari<sup>a</sup>, Abdul Malek Abdul Wahab<sup>a</sup>, Luqman Hakim Zulkifli<sup>a</sup>, Azmil Mohyidin<sup>a</sup>, Mat Hussin Ab Talib<sup>b</sup>, Intan Zaurah Mat Darus<sup>b</sup>

<sup>a</sup>Faculty of Mechanical Engineering, Universiti Teknologi MARA, 40450 Shah Alam, Selangor, Malaysia.

<sup>b</sup>Faculty of Mechanical Engineering, Universiti Teknologi Malaysia, 81310 UTM Johor Bahru, Johor, Malaysia.

## Article history

Received  
29<sup>th</sup> May 2025  
Revised  
31<sup>st</sup> October 2025  
Accepted  
31<sup>st</sup> October 2025  
Published  
2<sup>nd</sup> June 2026

\*Corresponding email: msukrihadi@uitm.edu.my

## ABSTRACT

*Vibration suppression in flexible structures is crucial for various engineering applications, including aerospace, robotics, and precision machinery. Passive vibration control approaches are effective for high-frequency applications, but often fail against low-frequency vibrations. Hence, active vibration control (AVC) is introduced to address this limitation. Among various AVC techniques, PID controller remains one of the most widely adopted methods. However, optimal tuning for PID parameters remains a challenge in complex dynamic systems. Therefore, this study explores the application of ant lion optimizer (ALO) to fine-tune PID parameters for vibration cancellation in a flexible structure. The optimization process is based on single objective function by minimizing the mean square error (MSE). Inspired by the predatory behaviour of antlions, ALO iteratively adjusts  $k_p$ ,  $k_i$ , and  $k_d$  values by updating the position of ants and antlions based on fitness evaluations. The performance of the PID-ALO controller is validated through MATLAB/ Simulink R2021a by assessing its effectiveness in attenuating vibrations induced by single and multiple sinusoidal disturbances. Results indicate that the PID-ALO controller outperformed the classical PID-ZN controller by achieving an attenuation level of 47.45 dB with 45.85% vibration reduction under single sinusoidal and 46.97 dB with 40.04% reduction under multiple sinusoidal disturbances. These findings highlight the potential of ALO in precise PID tuning, representing the first implementation of a PID-ALO controller on a horizontal flexible plate under dual excitation disturbances.*

**Keywords:** Active vibration control, Ant lion optimizer, Flexible structure, Metaheuristic algorithm, PID controller

© 2026 Penerbit UTM Press. All rights reserved

## 1.0 INTRODUCTION

Flexible structures have been a fundamental choice in engineering due to their durability, stability, and resistance to deformation under static and dynamic loads. Their strength makes them ideal for applications requiring high load-bearing capacity such as aeronautics, bridges, buildings and heavy machinery [1]. However, their rigidity limits adaptability in dynamic environments making rigid structures less suitable for applications that require flexibility and energy efficiency. Therefore, engineers have shifted toward flexible

structures which offer advantages in terms of lightweight design, economical and improved energy efficiency. Despite these benefits, flexible structures are highly prone to unwanted vibrations and may degrade the system performance and cause structural instability [2].

Managing excessive vibrations in flexible structures including plates, beams and manipulators, remains a critical challenge in engineering domains where precision and operational reliability are essential such as robotics, automotive systems and aerospace applications. These vibrations often arise from dynamic forces caused by poor system performance [3]. Hence, effective vibration suppression techniques are implemented to maintain system stability. Various vibration suppression techniques have been explored by researchers to address these challenges which broadly categorized into passive, active and hybrid methods [4]. Passive vibration control (PVC) has been widely employed in engineering applications by utilizing elements such as dampers, isolators, and viscoelastic materials to disseminate vibration without requiring external power [5].

These methods are particularly effective in attenuating high-frequency vibrations and are commonly integrated into aerospace, automotive and structural applications [6]. However, despite their reliability and ease of implementation, PVC techniques face significant limitations in handling low-frequency applications and adapting to dynamic environmental conditions. The inability to actively respond to different disturbances, coupled with added structural weight and a fixed operational bandwidth, ultimately restricts effectiveness in many modern applications [7]. Consequently, researchers have increasingly emphasized active vibration control (AVC) as an alternative to overcoming these challenges. Effective vibration suppression in active control systems depends on selecting an appropriate control strategy [8].

The proportional-integral-derivative (PID) controller remains a preferred choice due to its balance of simplicity, adaptability and reliability. The effectiveness of a PID controller is strongly influenced by the proper tuning of its proportional,  $k_p$ , integral,  $k_i$ , and derivative,  $k_d$  parameters as these directly impact system stability and performance [9]. Traditional tuning methods such as Ziegler Nichols (ZN) and Cohen Coon (CC) techniques have been widely adopted due to their straightforward implementation and empirical effectiveness [10]. For instance, the ZN method determines the PID gains by inducing sustained oscillations in the system and deriving parameters based on the ultimate gain and oscillation period [11]. While these methods offer a structured framework for PID tuning, they often lead to aggressive or suboptimal control responses, making them less effective for systems with complex dynamics, time delays or high-order behaviours [12].

Furthermore, classical techniques rely on empirical rules that may not generalize well across different applications, potentially compromising control accuracy and robustness [13]. These limitations have driven the exploration of more adaptive tuning strategies that can enhance PID controller performance in diverse and dynamic environments. Recently, researchers have increasingly adopted intelligent tuning approaches based on metaheuristic algorithms. Techniques such as particle swarm optimization (PSO), genetic algorithm (GA), bacterial foraging (BF) and mayflies optimization (MFO) offer a more flexible and efficient means of determining optimal PID parameters [14]. Unlike traditional methods that rely on trial-and-error adjustments, metaheuristic algorithms iteratively search for the best parameter combination by evaluating system performance against predefined cost functions [15].

These optimization-based approaches do not require an explicit mathematical model of the system, making them highly adaptable to nonlinearities and varying operating conditions. Studies have shown that PID controller tuned by metaheuristic algorithm achieved superior performance, provides faster response times, reduced overshoot and improved robustness compared to classical tuning techniques [6]. For instance, Li et al. (2023) successfully applied a PSO for PID tuning to enhance the performance of robotic manipulator [16]. Similarly, Sharma (2016) demonstrated the effectiveness of GA for

industrial process control as the result achieved faster response times and reduced overshoot [17].

These studies highlight the growing potential of metaheuristic in obtaining PID parameters to achieve optimal performance across various engineering applications. Hence, integrating intelligent tuning methods presents a promising solution for complex system. Over the past few years, the ant lion optimizer (ALO) has emerged as a promising metaheuristic algorithm for optimization problems [18]. ALO is introduced by Mirjalili (2015) by mathematically models key hunting stages, including random walks, trap construction, entrapment, prey capture and trap reconstruction. This algorithm is preferred to solve many application problems due to its ability to balance between exploration and exploitation during obtaining the optimum solution [19].

Pradhan et al. (2018) utilized ALO to tune PID controllers for an automobile cruise control system. The study showed that the PID-ALO achieved faster setting time, minimal overshoot and zero steady-state error compared to conventional methods [20]. Furthermore, George and Ganesan (2020) demonstrated the effectiveness of ALO in vibration suppression where significant disturbance rejection and system stability is achieved [21]. These applications highlight the growing relevance of ALO in engineering field which further reinforcing the role of metaheuristics algorithms in overcoming the limitations of traditional methods. Due to the successful implementation of ALO in previous studies, this research is motivated to adopt ALO for optimizing the PID controller parameters [20,21]. The algorithm has demonstrated its strong convergence characteristics, robust global search capability, and improved accuracy in avoiding local minima compared to other metaheuristic algorithms such as PSO, GA, and BF.

In this research, an intelligent PID controller optimized using the ant lion optimizer (ALO) algorithm is proposed to determine the optimal values of  $k_p$ ,  $k_i$ , and  $k_d$ . The objective is to achieve enhanced vibration suppression in flexible structures, particularly emphasis on reducing vibrations at the first mode. The system is modeled using a discrete transfer function derived from a simulation in MATLAB/ Simulink R2021a environment. This study presents the application of the Ant Lion Optimizer (ALO) for tuning PID controller parameters to achieve effective vibration suppression in flexible structures. It also provides a comprehensive performance evaluation of the PID-ALO controller under varying operational conditions and dynamic disturbances including both single and multiple sinusoidal inputs.

## 2.0 METHODOLOGY

### 2.1 System Modelling and Active Vibration Control

The system considered in this study is a flexible structure modelled using a discrete-time transfer function developed within the MATLAB/Simulink R2021a environment. Rather than relying on physical parameters such as mass or damping, the model is derived from system identification techniques based on the input-output behaviour of the structure. The transfer function used to model the flexible structure is based on the work of Raof et al. (2022), who derived it through system identification approach PSO [22]. This transfer function is represented in Equation (1) which denotes the system dynamic behaviour and serves as the plant for implementing the active vibration control strategy.

$$\frac{y(t)}{u(t)} = \frac{0.3843z^{-1} - 0.0022z^{-2}}{1 - 1.4138z^{-1} + 0.9931z^{-2}} \quad (1)$$

The objective of the model is to simulate vibration responses, particularly at the first mode, which is typically dominant in structures. To evaluate the robustness of the developed PID

controller, the system is excited using sinusoidal disturbances, namely single and multiple frequencies. The flexible plate system model was derived from experimentally obtained data, which accurately represents the dynamic behaviour of the actual structure [22]. Sinusoidal disturbances are widely employed in vibration control research to emulate periodic excitations commonly encountered in practical systems such as rotating machinery, actuators, or structural oscillations [21, 22]. They provide a controlled and repeatable means of assessing the ability of a controller to attenuate harmonic responses across specific frequency ranges.

The input-output behaviours presented in Figures 1(A) and 1(B) were obtained entirely from simulations conducted in MATLAB/ Simulink. In this setup, the system was excited using sinusoidal disturbances to evaluate the performance of the proposed PID-ALO controller. The ALO was employed to tune the PID parameters namely  $k_p$ ,  $k_i$  and  $k_d$  based on the lowest MSE. The optimization process iteratively adjusted these gains through feedback within the block diagram until the lowest MSE value was achieved. Initially, the tuning was performed under a single sinusoidal disturbance. The resulting optimal parameters were subsequently tested with multiple sinusoidal disturbances to validate controller performance.

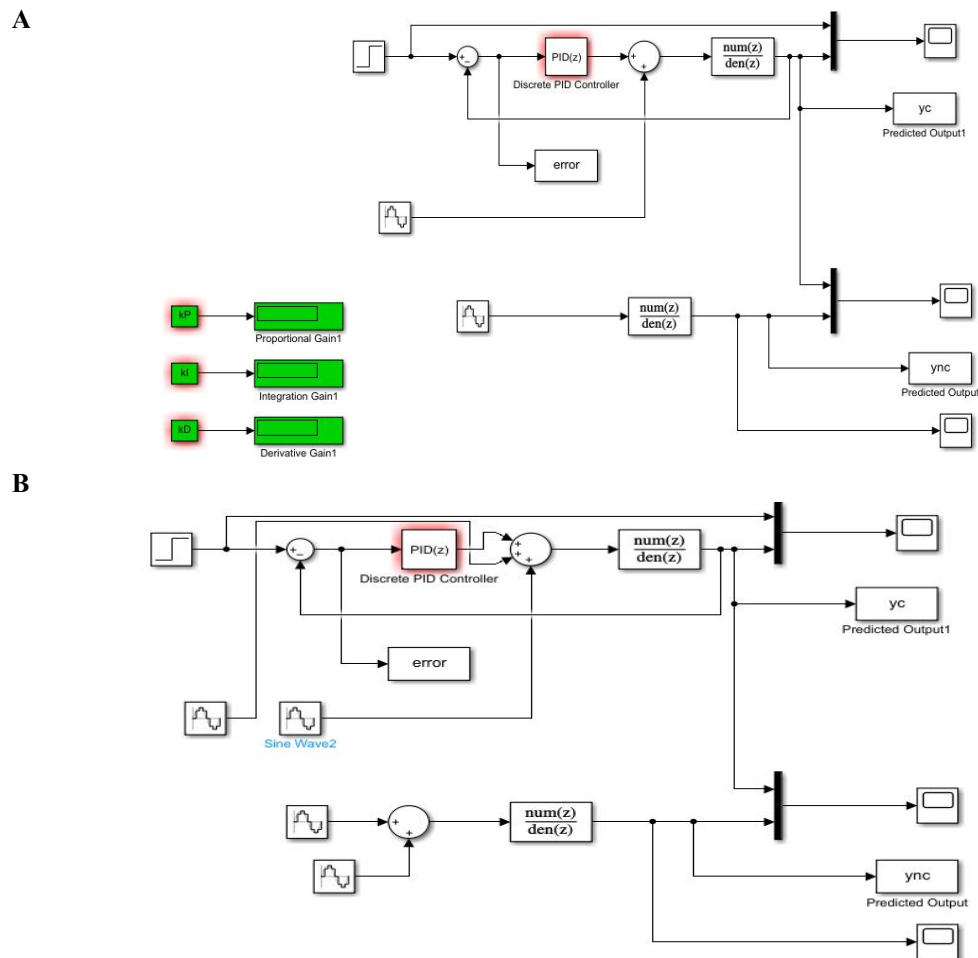


**Figure 1:** Development of block diagram under (A) single sinusoidal, (B) multiple sinusoidal disturbances

## 2.2 The Ant Lion Optimizer (ALO): Theory and Mechanism

Ant lion optimizer (ALO) is a nature-inspired metaheuristic algorithm based on the predatory behaviour of antlion larvae introduced by Mirjalili (2015). These larvae create conical sand pits to trap ants by exhibiting a blend of exploration and exploitation strategies that are key to their hunting success [19]. In the context of ALO, the “ants” represent candidate solutions and the “ant lions” represent optimal solutions. The algorithm operates by iteratively updating the positions of ants through random walks influenced by the best-performing antlions, which guide the search process towards an optimal solution. This mimicry of nature behaviour hunting strategies allows ALO to effectively balance the global and local searches by ensuring convergence to a global optimum while avoiding premature trapping in local minima [23].

ALO is structured around a series of steps that reflect the antlion hunting process. These steps include the random walks of ants, trap construction, entrapment, prey capture, and trap reconstruction. In the algorithm, ants move within the search space based on random walk strategies, and the antlions adjust the positions of the ants to guide them towards the optimal solution. These steps are repeated iteratively with the fitness of each solution evaluated through the fitness function to determine the effectiveness of the problem optimization. The concept behind ALO inspired by this natural behaviour is illustrated in Figure 2. The application of ALO algorithm has shown great promise, particularly for systems with complex and nonlinear dynamics including tuning of PID controller.

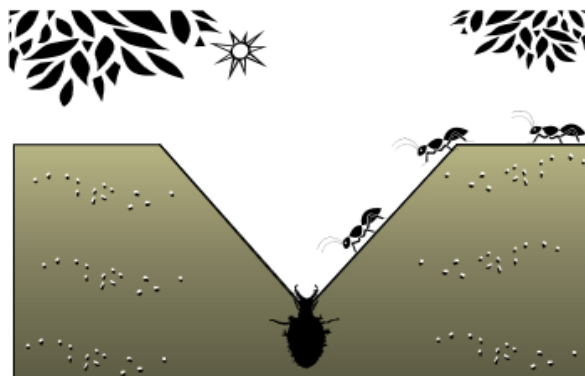


Figure 2: Antlion larvae waiting for ants to fall into the trap [23]

## 2.3 Implementation of ALO for PID Controller Tuning

This section outlines the optimization strategy employed to determine the optimal values of  $k_p$ ,  $k_i$ , and  $k_d$  using ALO. The primary objective is to minimize the MSE value between the desired and actual outputs, specifically targeting vibration attenuation at the first mode.

### Problem Formulation

#### Step 1: Initialization of ALO parameters and problem dimension

The algorithm begins with the initialization of four main parameters as follows:

- i) Number of ants ( $N_a$ )
- ii) Number of antlions ( $N_l$ )
- iii) Search space boundaries for each parameter (lower and upper bounds)
- iv) Maximum number of iterations ( $max_{gen}$ )

These parameters define the structure and exploration behaviour of the optimizer. For numerical purposes, let the initial parameter be as follows:

- i) Number of ants,  $N_a = 5$
- ii) Number of antlions,  $N_l = 5$
- iii) Search space boundaries:  
 $k_p \in [1, 10]$ ,  $k_i \in [0, 5]$ ,  $k_d \in [0, 2]$
- iv) Maximum number of iterations,  $max_{gen} = 10$

After that, the position of each ant and antlion are initialized uniformly at random within the predefined bounds. For illustration purposes, Tables 1 and 2 represent the random positions of ant and antlion, respectively. These values form the initial population from which the search for optimal PID gains begins.

**Table 1: Ant Random Positions Example**

Ant	$k_p$	$k_i$	$k_d$
1	4.20	2.75	1.50
2	8.10	1.30	0.95
3	6.35	0.90	0.45
4	2.80	3.85	1.80
5	9.00	2.10	1.10

**Table 2: Antlion Random Positions Example**

Antlion	$k_p$	$k_i$	$k_d$
1	5.50	2.00	1.00
2	7.75	1.20	1.50
3	3.25	4.00	0.80
4	6.00	0.75	0.50
5	4.00	3.20	1.25

Next, the PID gains for each ant is evaluated based on the objective function known as mean squared error (MSE). The MSE is defined in Equation (2):

$$MSE = \frac{1}{N} \sum_{i=1}^N (y_d(i) - y(i))^2 \quad (2)$$

where  $y_d(i)$  represents the predicted system output generated by the ant lion optimizer,  $y(i)$  denotes the actual system output obtained from the experiment, and  $N$  is the total number of time steps. The MSE was computed through MATLAB/ Simulink, with lower MSE values indicate better system performance. By assuming after simulation, the initial MSE values for ants are as presented in Table 3.

**Table 3: Fitness Evaluation for Initial Position**

Antlion	MSE
1	0.047
2	0.032
3	0.038
4	0.052
5	0.028 (best)

In this case, antlion 5 is considered the best solution as it achieved lowest value of MSE and is saved as the elite antlion to guide the rest of the optimization process.

**Step 2: Random walk and trapping mechanism**

Following the initialization phase, each ant in the population embarks on a stochastic exploration of the search space through a random walk. This movement is influenced simultaneously by two antlions which one selected using the roulette wheel selection method and the other being the elite antlion where it holds the best solution identified up to the current iteration. The roulette selection mechanism introduces diversity by probabilistically favouring fitter solutions, while the elite antlion serves as a convergence driver by guiding the ants toward optimal regions of the search space. This dual influence effectively balances exploration and exploitation during the optimization process. The random walk of each ant is modelled mathematically to mimic a cumulative one-dimensional stochastic motion. It is expressed by the Equation (3) [19]:

$$X(t) = [0, \text{cumsum}(2r(t_1) - 1), \text{cumsum}(2r(t_2) - 1), \dots, \text{cumsum}(2r(t_n) - 1)] \quad (3)$$

where *cumsum* denotes the cumulative sum operator, and *r(t)* represents a binary random function that generates either 0 or 1 depending on a uniformly distributed random number as shown in Equation (4) [19]:

$$r(t) = \begin{cases} 1, & \text{if } rand > 0.5 \\ 0, & \text{if } rand \leq 0.5 \end{cases} \quad (4)$$

This random binary output simulates the movement of ants either to the right (1) or to the left (0), cumulatively forming a random path over time. However, since the resulting walk can deviate beyond the permissible range or PID gains, a normalization process is applied to constraint the position within the dynamic bounds defined by the antlion trap. The normalization of the ants position at iteration *t* for each dimension *i* is performed using the Equation (5) [19]:

$$X_i^t = \frac{(X_i^t - a_i) \cdot (d_i^t - c_i^t)}{b_i^t - a_i} + c_i^t \quad (5)$$

where *a<sub>i</sub>* and *b<sub>i</sub>* represent the minimum and maximum values of the random walk-in dimension *i*, while *c<sub>i</sub><sup>t</sup>* and *d<sub>i</sub><sup>t</sup>* define the dynamic lower and upper bounds of the selected trap in that dimension. These bounds are derived from the selected antlion’s position, modulated by a time-dependent contraction factor that simulates the gradual narrowing of the trap as the optimization progress. To illustrate this mechanism numerically, consider ant 2 from the initial population with PID parameters *k<sub>p</sub>* = 8.10, *k<sub>i</sub>* = 1.30, and *k<sub>d</sub>* = 0.95.

Let it be influenced by

- a) Antlion selected by roulette wheel:

$$k_p = 5.50, \quad k_i = 2.00, \quad k_d = 1.00$$

- b) Elite antlion (best MSE):

$$k_p = 9.00, \quad k_i = 2.10, \quad k_d = 1.10$$

If the random walk for *k<sub>p</sub>* is 12 within bounds [-30, 30], and the trap is centred around 5.50 with range ±2, then,

$$X_{kp}^t = \frac{(12 - (-30)) \cdot (7.50 - 3.50)}{60} + 3.50 = 6.30$$

### Step 3: Adaptive trapping

As the optimization progresses, the search space is adaptively contracted to allow for finer exploitation around promising solutions. The dynamic bounds for each ant walk are updated using contraction coefficients which depends on the current iteration count  $t$  and total iterations,  $T$ . Equation (6) shows how antlions tighten their traps over time [19]:

$$c_i^t = l_i - \frac{l_i}{I(t)}, d_i^t = u_i + \frac{u_i}{I(t)} \quad (6)$$

where  $X_i$  is the current position of the selected antlion in dimension  $i$ , and  $c_i^t, d_i^t$  represent the dynamic lower and upper bounds, respectively. The time-dependent function  $I(t)$  governs the rate of contraction and is defined in Equation (7) [19]:

$$I(t) = 10^w \cdot \left(\frac{t}{T}\right) \quad (7)$$

where  $T$  is the maximum number of iterations,  $t$  is the current iteration index, and  $w \in [1,8]$  is a user-defined parameter that determines the degree of nonlinearity in the boundary reduction.

For adaptive trapping step, the numerical example can be illustrated by taking ant 2 which initially have values of 8.10, 1.30 and 0.95 for  $k_p, k_i$  and  $k_d$ , respectively. Assuming the current iteration,  $t = 5$ , and ant 2 is influenced by previously mentioned roulette-selected and elite antlion at step 2. Hence, by applying contraction formula in Equation (6):

$$c_{kp}^t = 5.50 - \frac{5.50}{5} = 4.40,$$

$$d_{kp}^t = 5.50 + \frac{5.50}{5} = 6.60$$

Similarly, for  $k_i$  and  $k_d$ ,

$$c_{ki}^t = 2.00 - \frac{2.00}{5} = 1.60,$$

$$d_{ki}^t = 2.00 + \frac{2.00}{5} = 2.40$$

$$c_{kd}^t = 1.00 - \frac{1.00}{5} = 0.80,$$

$$d_{kd}^t = 1.00 + \frac{1.00}{5} = 1.20$$

### Step 4: Elite antlion guidance

In addition to a randomly selected antlion, each ant is influenced by the elite antlion where the best solution identified so far. This dual-guidance strategy balances the global search with targeted exploitation of high-fitness regions. The final position of each ant is computed by averaging its normalized walks influenced by the roulette-selection and the elite antlions. The combination is given by Equation (8) [19]:

$$X_{new} = \frac{X_{RW-selected} + X_{RW-elite}}{2} \quad (8)$$

This step ensures ants gravitate toward optimal regions while retaining sufficient diversity. For example, when ant 2 undergo two random walks mentioned in step 2, the averaged new position is calculated using Equation (8):

$$k_p = \frac{6.30 + 8.20}{2} = 7.25 \quad k_i = \frac{1.90 + 2.00}{2} = 1.95 \quad k_d = \frac{1.05 + 1.00}{2} = 1.025$$

**Step 5: Boundary handling**

To ensure feasibility, any ant positions exceeding the PID gain bounds are corrected using boundary control. If a gain value  $k$  violates its bound  $[k_{min}, k_{max}]$ , it is clipped as follows [19]:

$$k = \begin{cases} k_{min} & \text{if } k < k_{min} \\ k_{max} & \text{if } k > k_{max} \\ k & \text{otherwise} \end{cases}$$

This step prevents invalid solutions and maintains the integrity of the PID parameter search. From previous calculations, all values obtained are within bounds, hence, no adjustment is needed.

$$k_p \in [1, 10]$$

$$k_i \in [0, 5]$$

$$k_d \in [0, 2]$$

**Step 6: Fitness evaluation and memory update**

After boundary correction, the new position of ants is evaluated based on the same fitness function which is MSE. If new MSE is better than its corresponding antlion MSE, the antlion position is replaced. The elite antlion is also updated if a better-performing ant is found. This memory update preserves the best solutions across generations and guides the swarm toward optimal PID gains. Assume the new MSE for Ant 2 is computed as 0.025. By comparing this value with the current MSE of the antlion it was associated with which is 0.032. Since the new value is better, hence, update the antlion position with the ant position. If 0.025 is also better than the elite which previously obtained as 0.028, then this becomes the new elite antlion.

**Step 7: Iterative optimization**

Steps 2 through 7 are repeated for the predefined number of iterations,  $max_{gen}$ . With each cycle, the population becomes more refined and the MSE values tend to converge. Table 4 highlights how the elite solution improves over iterations. Upon completing all iterations, the algorithm outputs the best performing PID parameters that achieve the minimum MSE are 7.85, 1.95 and 0.90 for  $k_p$ ,  $k_i$  and  $k_d$ , respectively. Figures 3 and 4 highlight the pseudocode of the ALO algorithm and block diagram utilized for PID controller tuning.

**Table 4:** Numerical Example to Achieve Optimum Solution at Maximum Iteration

Iteration	Best MSE	$k_p$	$k_i$	$k_d$
1	0.028	9.00	2.10	1.10
2	0.024	8.70	2.00	1.05
...	...	...	...	...
10	0.015 (final)	7.85	1.95	0.90

1. **Initialize** the positions of  $N_a$  and  $N_l$  randomly within the search space
2. **Evaluate** the fitness of all ants and antlions using MSE
3. **Identify** the elite antlion,  $X_{RW-elite}$  with the best fitness

4. **Repeat** for  $t = 1$  to  $max_{gene}$
5.     **For** each ant  $i = 1$  to  $N_a$  do
6.         **Select** an antlion via roulette wheel selection based on antlion fitness
7.         **For** each dimension  $k=1$  to  $D$  do
8.             **Update** the lower and upper bounds based on iteration  $t$
9.             **Generate** random walk  $X_{RW-selected}$  around selected antlion  $X_{RW-elite}$
10.            **Generate** random walk  $X_{RW-elite}$  around elite antlion  $X_{RW-selected}$
11.            **Normalize** both walks within the updated bounds
12.            **Update** the ant position as in Equation (8)
13.         **End for**
14.     **End for**
15. **Evaluate** the fitness values for all updated ants
16. **Replace** any antlion with the corresponding ant if the ant has better fitness
17. **Update** the elite if a new antlion has better fitness than the current elite
18. **End repeat**

**Figure 3:** Pseudocode of the ALO algorithm utilizes for PID controller tuning [19]

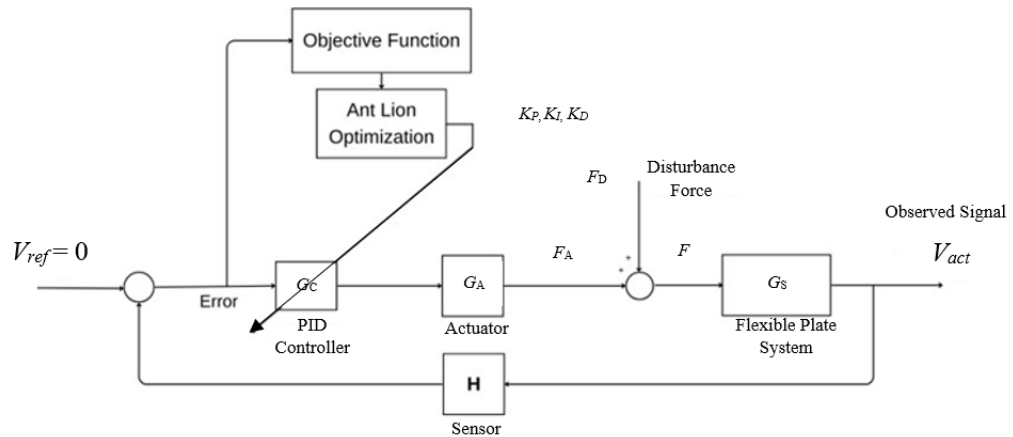


**Figure 4:** Block diagram of ALO implementation for PID controller tuning

### 3.0 RESULTS AND DISCUSSION

This section evaluates the performance of the PID controller optimized using the Ant Lion Optimizer (ALO) under both single and multiple sinusoidal excitation conditions. The classical Ziegler–Nichols (ZN) tuning method is employed as a benchmark for comparison. The robustness of the proposed controller is assessed through simulations conducted in MATLAB/Simulink R2021a across a range of excitation scenarios. As noted by Liu et al. (2023), attenuation of the first vibration mode is particularly important, as it predominantly influences the overall dynamic response of flexible structures [24]. Suppression of this mode often facilitates the mitigation of higher-order modes due to the redistribution of vibrational energy across the structure [25]. Accordingly, the present analysis focuses on the attenuation level of the first mode as a key performance indicator.

#### 3.1 PID-ALO under Single Sinusoidal Disturbance.

The effectiveness of ALO in fine-tuning PID gains relies heavily on the careful selection and adjustment of its key parameters. Based on the literature review, previous studies have demonstrated variability in the parameter setting used for optimization algorithms [26]. Four key parameters are considered for tuning in this study known as the number of ants,

the number of antlions, the lower and upper search boundaries and the number of iterations. Each parameter is systematically varied to enhance the controller’s performance in suppressing vibrations, with a particular focus on minimizing response magnitude and overall mean squared error (MSE).

In the initial tuning stage, the number of ants and antlions is optimized concurrently. These two parameters are set to identical values, which is standard practice in ALO-based algorithms [27]. This configuration maintains a balance between the foraging agents (ants) and their predators (antlions), a critical aspect of population-based metaheuristics. While ants contribute to global search diversity, antlions enhance local search exploitation [28]. According to Wang and Zhou (2024), a population size of 30 is sufficient to ensure diversity and to mitigate the risk of premature convergence to local optima [29]. Based on this guidance, the study evaluates population sizes ranging from 30 to 100 in increments of 10. Among these, a value of 50 for both ants and antlions demonstrates the most effective vibration suppression, achieving the lowest decibel magnitude and mean squared error (MSE). Following this result, the population size is fixed at 50 for subsequent parameter tuning stages.

Once the optimal number of ants and antlions is established, the lower and upper boundaries for the PID gain parameters are tuned. These boundaries define the permissible search space for the optimizer. If the range is too narrow, the optimizer may miss optimal solutions; conversely, overly broad ranges can slow convergence or result in unstable controller behavior [30]. In this study, the selection of boundary values for tuning  $k_p$ ,  $k_i$ , and  $k_d$  is informed by prior research that employed similar ranges for PID gain optimization [20, 21, 31]. Following preliminary trials, the most effective performance is achieved using the boundaries proposed by George and Ganesan (2020), with lower bounds of [0, 0, 0] and upper bounds of [50, 10, 5] for  $k_p$ ,  $k_i$ , and  $k_d$ , respectively. This configuration not only reduces vibration magnitude but also yields a significantly lower mean squared error (MSE). Within the ALO framework, well-defined boundary constraints are essential, as they guide the stochastic movement of ants around selected antlions during the trapping phase, thereby enhancing convergence behavior and improving the precision of PID parameter optimization [32].

The final tuning stage involves adjusting the number of iterations, which defines the total number of search cycles performed by the ALO algorithm. This parameter plays a critical role in determining both convergence speed and solution quality. An insufficient number of iterations may lead to premature convergence on suboptimal solutions, while an excessively high iteration count can increase computational overhead without delivering meaningful gains in accuracy [33]. To identify an optimal balance, iteration values ranging from 25 to 60 are tested. Empirical results indicate that 50 iterations offer the best trade-off between computational efficiency and optimization accuracy. This observation is consistent with the findings of Okwu and Tartibu (2021), who reported that the standard ALO algorithm typically reaches the optimal fitness region within approximately 41 iterations [34]. Similarly, Rajakumar et al. (2025) observed convergence in just 42 iterations for optimal wind turbine (WT) system placement [35]. Table 5 summarizes the final ALO parameter settings used for PID controller optimization. Based on this configuration, the optimal values of  $k_p$ ,  $k_i$ , and  $k_d$  are obtained, as listed in Table 6. These gains produce the most effective vibration suppression and the lowest mean squared error (MSE) observed in the study.

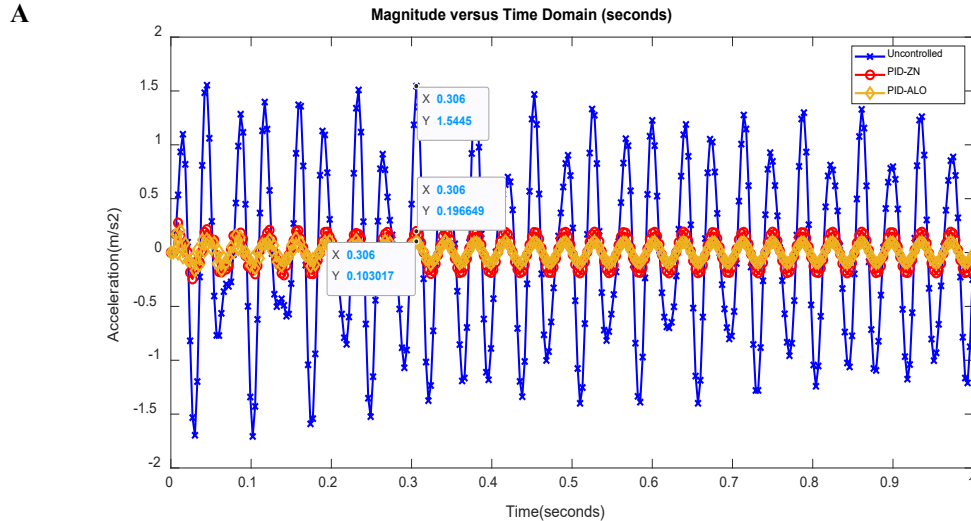
**Table 5:** The Best Value of Parameters Achieved for PID-ALO

Parameters	Values
Number of ants	50
Number of antlions	50
Lower boundaries	[0, 0, 0]
Upper boundaries	[50, 10, 5]
Maximum iteration	50

**Table 6: PID-ALO Parameters Setting for Vibration Suppression**

Controller	$k_p$	$k_i$	$k_d$
Uncontrolled	-	-	-
PID-ALO	8.0445	2.8358	0.0111

The effectiveness of the proposed PID-ALO controller is evaluated by comparing its performance with that of the classical Ziegler–Nichols (ZN) tuning method. The PID-ZN controller is developed using the same transfer function and disturbance characteristics employed in previous studies. Specifically, the ZN tuning parameters are adopted from the study by Hadi et al. (2018), where the ultimate gain,  $k_{cr}$  is identified as 6.5 and the corresponding ultimate oscillation period,  $p_{cr}$  was determined to be 0.036s. These values are substituted into the classical ZN tuning formulas to calculate the PID gains, resulting in  $k_p = 3.9$ ,  $k_i = 0.02$ , and  $k_d = 0.005$  [36]. In contrast, the PID-ALO approach yields significantly refined gain values of  $k_p = 8.0445$ ,  $k_i = 2.8358$ , and  $k_d = 0.0111$ . In terms of vibration suppression, the uncontrolled system exhibits a peak magnitude of 103.50 dB. The PID-ZN controller reduces this to 69.13 dB, achieving an attenuation of 34.37 dB at the first mode and a vibration reduction of 33.21%. The PID-ALO controller further improves performance, reducing the magnitude to 56.05 dB corresponding to an attenuation of 47.45 dB and a 45.85% reduction in vibration. Additionally, the mean squared error (MSE) decreases substantially from 0.0183 with the PID-ZN controller to 0.0055 with the PID-ALO controller. A summary of the PID tuning results under single sinusoidal input excitation is provided in Table 7. A detailed comparison of the system responses in both time and frequency domains is illustrated in Figure 5(A) and Figure 5(B), respectively, highlighting the enhanced suppression achieved by the PID-ALO controller, particularly at the first mode of vibration.



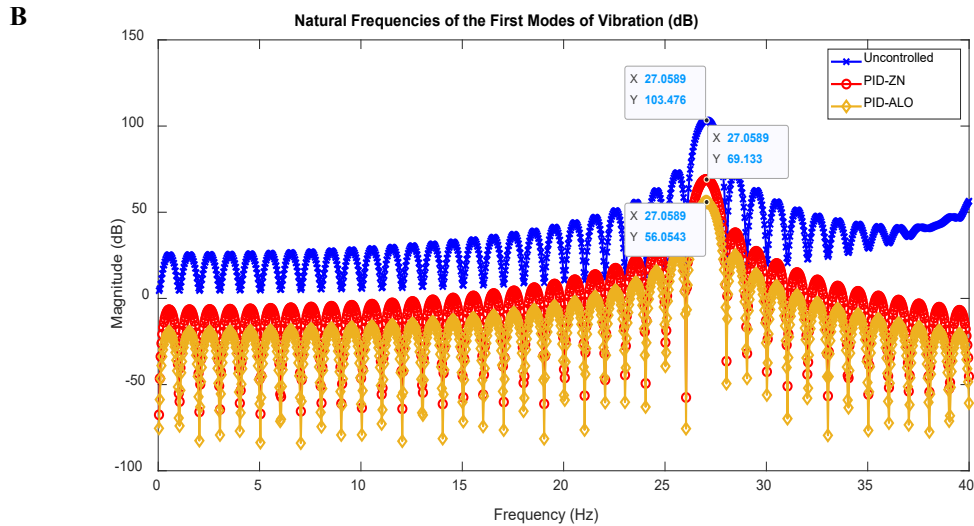


**Figure 5:** System response under single sinusoidal disturbance for PID-ZN and PID-ALO controller in (A) time-domain, (B) frequency-domain

**Table 7:** Performance Comparison of PID-ZN and PID-ALO Under Single Sinusoidal Input

Controller	Uncontrolled	PID-ZN [36]	PID-ALO
PID gains obtained	-	$k_p = 3.9$ $k_i = 0.02$ $k_d = 0.005$	$k_p = 8.0445$ $k_i = 2.8358$ $k_d = 0.0111$
Decibel magnitude (dB)	103.50	69.13	56.05
First mode attenuation level (dB)	Reference	34.37	47.45
Vibration reduction (%)	Reference	33.21	45.85%
MSE value	0.6655	0.0183	0.0055

### 3.2 PID-ALO under Multiple Sinusoidal Disturbance.

To further evaluate the robustness and adaptability of the proposed controllers, the system is subjected to multiple sinusoidal disturbances using the same PID gains identified in the previous case. The performance of the PID-ZN and PID-ALO controllers under these conditions is analyzed and compared. The PID-ZN controller achieves an attenuation of 34.34 dB in the first mode, corresponding to a 29.24% reduction in vibration amplitude. In contrast, the PID-ALO controller outperforms the PID-ZN method by achieving a higher attenuation of 46.97 dB, which corresponds to a 40.04% vibration reduction. These results indicate that the PID-ALO controller provides superior vibration suppression under multiple sinusoidal disturbances compared to the classical ZN-tuned controller. A summary of this comparison is provided in Table 8. Additionally, the system responses in both time and frequency domains are illustrated in Figures 6(A) and 6(B), respectively.

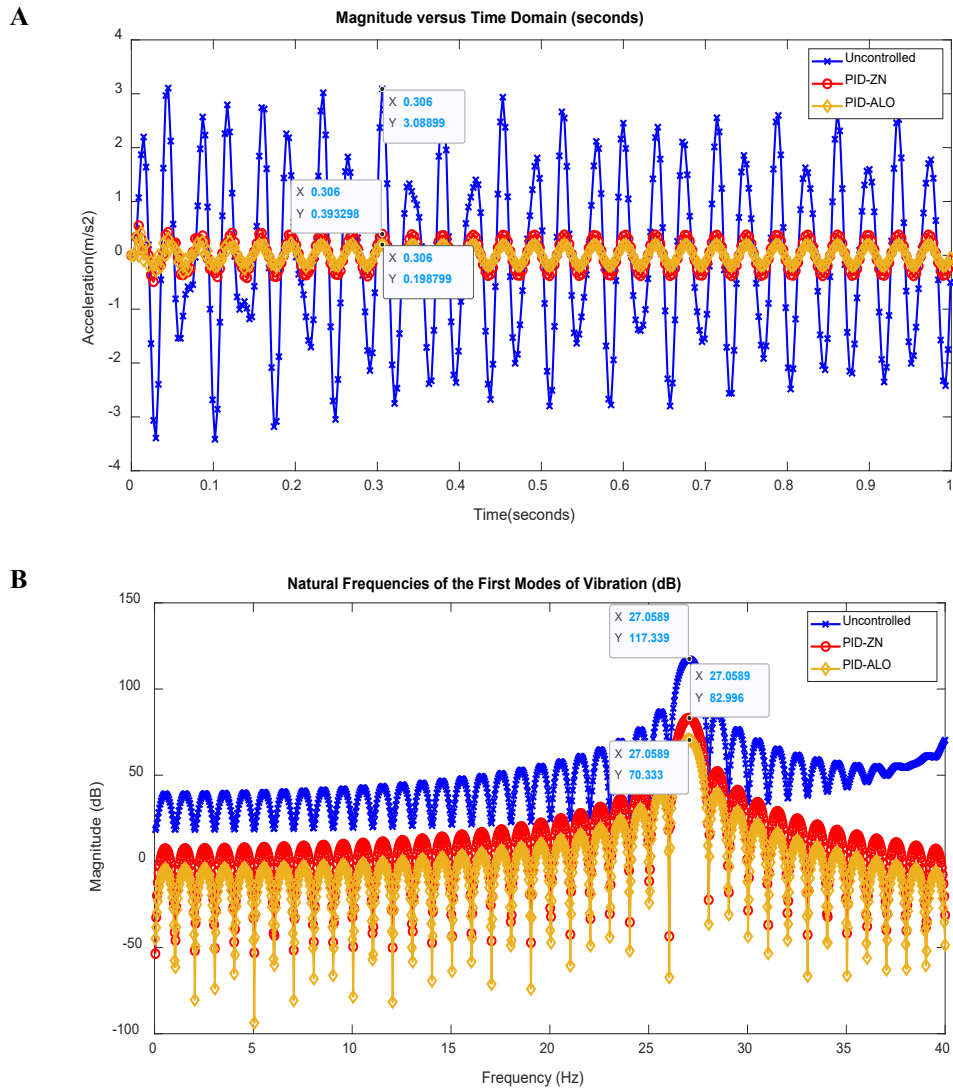


**Figure 6:** System response under multiple sinusoidal disturbance for PID-ZN and PID-ALO controller in (A) time-domain, (B) frequency-domain

**Table 8:** Performance Comparison of PID-ZN and PID-ALO Under Multiple Sinusoidal Input

Controller	Uncontrolled	PID-ZN [36]	PID-ALO
PID gains obtained	-	$k_p = 3.9$ $k_i = 0.02$ $k_d = 0.005$	$k_p = 8.0445$ $k_i = 2.8358$ $k_d = 0.0111$
Decibel magnitude (dB)	117.30	83.00	70.33
First mode attenuation level (dB)	Reference	34.34	46.97
Vibration reduction (%)	Reference	29.24	40.04%
MSE value	0.6656	0.0183	0.0055

### 3.3 Comparative Performance Analysis

The improved performance of the PID-ALO controller is attributed to its global optimization capability which allows it to explore the solutions space more comprehensively than heuristic methods like ZN. Unlike ZN approach which is optimized for a specific frequency or transient response, ALO adaptively tunes the PID gains to reduce

vibration amplitudes across a broader frequency spectrum. Furthermore, ALO employs adaptive tuning mechanisms, including stochastic random walks and elitism-based selection which allow the controller to adjust dynamically and response effectively to complex disturbances. These adaptive properties are particularly beneficial in various types of disturbance environments where fixed-gains methods often struggle to maintain consistent performance. Furthermore, the robustness of the PID-ALO controller is evident in its ability to sustain high attenuation across diverse excitation modes, hence highlighting its suitability for practical systems with unpredictable disturbance characteristics.

The performance gap between PID-ALO and PID-ZN becomes more pronounced under these demanding conditions, indicating that ALO not only matches but excels in complex scenarios. This robustness and adaptability make ALO a compelling choice for real-world vibration suppression applications. These advantages align with prior studies that utilized other metaheuristic algorithms such as social spider optimization (SSO), bird mating optimizer (BMO), and the advanced firefly algorithm (AFA) where all of which report improved control performance in horizontal flexible structures [37-39].

For reference, Hadi et al. (2018) applied a PID-PSO controller for the same horizontal flexible plate system and achieved an attenuation of 47.28 dB at the first vibration mode [36]. In this study, the proposed PID-ALO controller achieved comparable attenuation levels of 47.45 dB under single and 46.97 dB under multiple sinusoidal disturbances. This similarity validates the capability of ALO as an alternative metaheuristic algorithm for PID parameter optimization. The consistent results obtained across multiple algorithms reaffirm the superiority of metaheuristic for optimization of PID tuning over conventional approaches. Hence, emphasized their robustness, adaptability, and potential for real-world vibration suppression applications.

#### 4.0 CONCLUSION

This study investigates the effectiveness of tuning a PID controller using the Ant Lion Optimizer (ALO) algorithm for vibration suppression in a horizontal flexible plate structure under both single and multiple sinusoidal disturbances. The performance of the PID-ALO controller was thoroughly evaluated in both time and frequency domains and compared against the classical PID-ZN controller to assess its superiority. Under the single sinusoidal input, the PID-ALO controller achieved a first mode attenuation of 47.45 dB, corresponding to a 45.85% vibration reduction. For multiple disturbances, it achieved 46.97 dB attenuation with a 40.04% reduction. In contrast, the PID-ZN controller recorded 34.37 dB and 33.21% reduction for single sinusoidal input, and 34.34 dB with 29.24% for multiple disturbances. In both scenarios, the PID-ALO controller outperformed the classical method in terms of vibration suppression and mean squared error, demonstrating strong optimization capability and robust control performance. However, the stochastic nature of ALO may introduce additional computational effort and lead to slight performance variability between runs. Despite these limitations, the algorithm shows strong potential for further enhancement through hybrid or adaptive optimization methods such as combining ALO with PSO to improve convergence efficiency. The approach presented in this study can also be extended to higher-degree-of-freedom or multi-input-multi-output (MIMO) systems to evaluate the scalability and effectiveness of ALO in more complex vibration environments. Future work will focus on implementing the PID-ALO controller on experimental platforms with increased structural complexity to further validate its performance and adaptability.

## ACKNOWLEDGEMENT

The authors gratefully acknowledge Universiti Teknologi MARA (UiTM), Universiti Teknologi Malaysia (UTM), and the Ministry of Higher Education (MoHE) for their financial support and for providing the necessary facilities to conduct this research.

## REFERENCES

1. Farghani M, Soltanaghaei M, Zamani ZB. Dynamic optimization scheme for load balancing and energy efficiency in software-defined networks utilizing the krill herd meta-heuristic algorithm. *Computers and Electrical Engineering*. 2024;114(C).
2. Rawi NNM, Hadi MS. Parameter identification of horizontal flexible plate system using cuckoo search algorithm. In *Recent Trends in Mechatronics Towards Industry 4.0*. 2022;730:205-217.
3. Warke V et al. Improving the useful life of tools using active vibration control through data-driven approaches: A systematic literature review. In *Eng. Appl. Artif. Intell.* 2024;28.
4. Hadi MS, Mat Darus IZ, Tokhi MO, Jamid MF. Active vibration control of a horizontal flexible plate structure using intelligent proportional–integral–derivative controller tuned by fuzzy logic and artificial bee colony algorithm. *Journal of Low Frequency, Noise, Vibration and Active Control*. 2020;39(4): 1159-1171.
5. Luo DY, Cheng B, Wu B, Wang XL, Lin Q. design of an active low frequency vibration isolation system for atom interferometry by using sliding mode control. *Civ. Eng. J.* 2017;26(4).
6. Zamri MIA, Hadi MS, Shaari ANS, Mokhtar NM. Proportional integral derivative controller based on ant colony optimization for vibration cancellation of horizontal flexible plate structure. *Int. J. Electr. Comput. Eng. IJECE*. 2022;12(4):3583–2594.
7. Jamalabadi MYA. Active control of submerged systems by moving mass. *Acoustics*. 2021;3(1):42–57.
8. Jamali A, Mat Darus IZ, Tokhi MO. Intelligent PID controller of flexible link manipulator with payload. In *3rd International Conference on Mechanical, Electronics, Computer, and Industrial Technology (MECnIT)*. 2020;118–122.
9. Li Z. Review of PID control design and tuning methods. *J. Phys. Conf. Ser.* 2023;2649(1).
10. Tasoren AE. Design and realization of online auto tuning PID controller based on cohen-coon method. *Eur. J. Sci. Technol.* 2021;24:35–239.
11. Baz A. On the ziegler destabilization paradox. *Acta Mech.* 2025; 236(4):2445–2461.
12. Khodja MA, Tadjine M, Boucherit MS, Benzaoui M. Tuning PID attitude stabilization of a quadrotor using particle swarm optimization (experimental). *Int. J. Simul. Multidiscip. Des. Optim.* 2017;8:1–9.
13. Safiullah, Joshi A, Hote YV. Practical and comparative analysis of PID tuning and ADRC variants with communication delay. In *2022 34th Chinese Control and Decision Conference (CCDC)*. 2022:3858–3863.
14. Ma X, Deng H. Bacterial foraging optimization algorithm with dynamically reduced setting of migration probability. In *2021 The 13th International Conference on Computer Modeling and Simulation*. 2021: 251–257.
15. Hussain K, Mohd Salleh MN, Prasetyo YA, Cheng S. personal best cuckoo search algorithm for global optimization. *Int. J. Adv. Sci. Eng. Inf. Technol.* 2018;8(4).
16. Li W, Cui J, Bian X, Zou L. Velocity feedback control method of low-frequency electromagnetic vibration exciter based on kalman filter estimation. In *Rev. Sci. Instrum.* 2023;94(3).
17. Sharma S. Application of genetic algorithm in software engineering distributed computing and machine learning. *Int. J. Comput. Appl. Inf. Technol.* 2016;9(2):208–212.
18. Guo MW, Wang JS, Zhu LF, Guo SS, Xie W. Improved ant lion optimizer based on spiral complex path searching patterns. In *IEEE Access*. 2020;8:22094–22126.
19. Mirjalili S. The ant lion optimizer. *Adv. Eng. Softw.* 2015; 83: 80-98.
20. Pradhan R, Majhi SK, Pradhan JK, Pati BB. Antlion optimizer tuned PID controller based on bode ideal transfer function for automobile cruise control system. In *J. Ind. Inf. Integr.* 2018;9:45-52.
21. George T, Ganesan V. An effective technique for tuning the time delay system with PID controller-ant lion optimizer algorithm with ANN technique. In *Int. J. Eng. Adv. Technol.* 2020;9(3):2421-2429.
22. Raof AIA, Hadi MS, Jamali A, Mohd Yatim H, Ab Talib MH, Mat Darus IZ. Intelligent PID controller tuned by bacterial foraging optimization algorithm for vibration suppression of horizontal flexible structure. In *2022 IEEE 8th International Conference on Smart Instrumentation, Measurement and Applications (ICSIMA2022)*. 2022; 237-241.
23. Assiri AS, Hussien, AG, Amin M. ant lion optimization: variants, hybrids, and applications. In *IEEE Access*. 2020;8:77746–77764.
24. Liu G, Zhou P, Yu T, Li Z. Optimal design of nonlinear negative-stiffness damper with flexible support for mitigating cable vibration. *Buildings*. 2023;13(10):1–18.
25. Yang S, Fan W, Liu Y, Lai K, Chen B, Chen Z. Performance of a novel magnetic stiffness-adjustable wire rope damper in high-mode vibration control of cables. *J. Bridge Eng.* 2025;30(5).

26. Guo H. Research on ant lion optimization algorithm for BP neural network in transformer fault diagnosis. In *J. Big Data Comput.* 2024;2(3):1–5.
27. Aziz MAA, Mat Yasin Z, Zakaria Z. enhancing optimal unit commitment via ant lion optimizer with photovoltaic uncertainty. In *PaperASIA.* 2025;41(3b):156–166.
28. Zade BMH, Mansouri N, Javidi MM. A new hyper-heuristic based on ant lion optimizer and tabu search algorithm for replica management in cloud environment. In *Artif. Intell. Rev.* 2023;56(9): 9837–9947.
29. Wang W, Zhou R. Application of improved ant-lion algorithm for power systems. In *PLOS ONE.* 2024;19(12):1–22.
30. Fathi IS, Abo Bakr RM, Farouk RM. Some penalty-based constraint handling techniques with ant lion optimizer for solving constrained optimization problems. *Int. J. Comput. Appl.* 2024;181(30):24–36.
31. Pradhan R, Majhi SK, Pradhan JK, Pati BB. Optimal fractional order PID controller design using ant lion optimizer. *Ain Shams Eng. J.* 2020;11(3):281–291.
32. Ning Y, Minglei R, Shuai G, Guohua L, Bin H, Xiaoyang L, Rong T. An advanced multi-objective ant lion algorithm for reservoir flood control optimal operation. *Water.* 2024;16(6):1-13.
33. Mat Yasin Z, Sam'on IN, Mohamad H, Ab Wahab N. Optimal under-voltage load shedding using ant lion optimizer. *Int. J. Simul. Syst. Sci. Technol.* 2017;17(41):1–6.
34. Okwu MO, Tartibu LK. Ant lion optimization algorithm. In *Metaheuristic Optimization: Nature-Inspired Algorithms Swarm and Computational Intelligence, Theory and Applications.* 2021;927: 85–94.
35. Rajakumar P, Balasubramaniam PM, Aldulaimi MH, Arunkumar M, Ramesh S, Alam MM, Al-Mdallal QM. An integrated approach using active power loss sensitivity index and modified ant lion optimization algorithm for DG placement in radial power distribution network. *Sci. Rep.* 2025;15(1): 1–27.
36. Hadi MS, Mohd Yatim H, Mat Darus IZ. Modelling and control of horizontal flexible plate using particle swarm optimization. *Int. J. Eng. Technol.* 2018;7(2.29).
37. Hadi MS, Lotpi AFH, Yatim HM, Ab. Talib MH, Mat Darus IZ. PID controller optimized by bird mating optimizer for vibration control of horizontal flexible plate. In *Intelligent Manufacturing and Mechatronics.* 2024;850:303–313.
38. Yatim HM, Ab Talib MH, Mat Darus IZ, Zahari ZI, Hadi MS. Advanced firefly algorithm (AFA) for PID controller of flexible horizontal plate structure. In *2024 IEEE 10th International Conference on Smart Instrumentation, Measurement and Applications (ICSIMA).* 2024;201–206.
39. Hadi MS, Hekim LKJ, Jamali A, Mat Darus IZ, Tokhi MO. Intelligent PID controller for vibration suppression of horizontal flexible plate based on social spider optimization. In *Walking Robots into Real World.* 2024;1115:183–192.